



Experimental and Computational Fluid Dynamics Simulation Study on the Performance of a Two-stroke Aviation Engine: A Comparative Analysis of Turbulence Models and Mesh Strategies

G. Coskun^{1†}, Y. Delil¹ and U. Demir²

¹Department of Mechanical Engineering, Sakarya University, Sakarya, Turkey

²Department of Mechanical Engineering, Bilecik Şeyh Edebali University, Bilecik, Turkey

†Corresponding Author Email: gcuskun@sakarya.edu.tr

ABSTRACT

This study presents an experimental and computational fluid dynamics (CFD) analysis to evaluate the performance of a two-stroke aviation engine under constant operating conditions. The experiments were conducted at 4800 RPM and full load, where high-precision measurement devices recorded critical performance parameters, including total mass flow rate, fuel mass flow rate, torque, volumetric efficiency, and in-cylinder pressure and temperature. For CFD analysis, a three-dimensional combustion chamber model of the engine was developed, and two turbulence models (Standard k- ϵ and RNG k- ϵ) were employed using three different mesh sizes (2 mm, 3 mm, and 4 mm). The numerical results were compared with experimental data to determine the most accurate simulation configuration. The findings indicate that decreasing the mesh size improves the accuracy of the simulations, with the Standard k- ϵ model using a 2 mm mesh producing the most precise predictions across multiple parameters. The error rate for total mass flow rate and volumetric efficiency was reduced to 9%, demonstrating the effectiveness of fine mesh resolution. However, the RNG k- ϵ model yielded better accuracy for specific fuel consumption, achieving a 0.1% error rate at a 2 mm mesh size. Velocity and temperature distributions revealed that flow gradients were more accurately captured with smaller mesh sizes, particularly in the bypass and exhaust port regions. The Standard k- ϵ model was more effective in predicting in-cylinder pressure and heat release characteristics, while the RNG k- ϵ model predicted slightly higher maximum in-cylinder temperatures. Mesh refinement significantly influenced combustion behavior, with smaller mesh sizes leading to more accurate heat transfer and reaction modeling. Overall, this study highlights the impact of mesh size selection and turbulence modeling on CFD-based performance analysis of two-stroke aviation engines. The results provide valuable insights for optimizing CFD modeling strategies and can serve as a reference for future research on engine design, performance enhancement, and computational accuracy improvements.

Article History

Received December 28, 2024
Revised February 25, 2025
Accepted April 3, 2025
Available online June 3, 2025

Keywords:

Two-stroke engine
Computational fluid dynamics
Combustion simulation
Adaptive mesh refinement
Turbulence model

1. INTRODUCTION

Aviation has witnessed an unprecedented evolution in the last century (Sehra & Whitlow, 2004). With this evolution has come an ever-increasing demand for more efficient, compact, and lightweight engine systems (Benini, 2011). Fuel efficiency and the engine's total weight pivotal roles in aviation vehicles' overall performance and operational economic especially when evaluating their total flight duration (Epstein, 2014).

Furthermore, the impact of emissions and environmental damage are becoming important issues nowadays (Korba et al., 2023).

Among the different types of internal combustion engines (ICE), two-stroke engines have become particularly significant in the domain of small aviation vehicles (Cantore et al., 2014). Their inherent advantage lies in their compact design and lower weight, which offer better power-to-weight ratios when compared to their four-stroke counterparts (Mikalsen & Roskilly, 2008).

NOMENCLATURE			
<i>AMG</i>	Automatic Mesh Generation	<i>CFD</i>	Computational Fluid Dynamic
<i>aTDC</i>	After Top Dead Center	<i>HRR</i>	Heat Release Rate
<i>bTDC</i>	Before Top Dead Center	<i>ICE</i>	Internal Combustion Engine
<i>CAD</i>	Crank Angle Degree	<i>RPM</i>	Revolutions Per Minute

This makes them highly preferable for aircraft where weight and space are at a premium (Cleveland, 2012). Yet, for all their advantages, two-stroke engines present unique challenges in terms of modeling and simulation (Bozza et al., 1995; Turesson, n.d.).

The world of computational simulations has made significant strides, particularly with the advent of Computational Fluid Dynamics (CFD) (Tu et al., 2018). Today CFD simulation software offers significant convenience in the field of four-stroke engines. Modeling valve movements is no longer as complex as in older versions, and error rates during simulation have been significantly reduced. Even it is important to model intake period for some injection strategies a closed-cycle period without accounting for dynamic valve movements can simplified the process considerably (Demir et al., 2022a; Wang et al., 2002). Unfortunately, it is not valid for two-stroke engines. Given their operational mechanics, simulating the intake and exhaust periods is unavoidable, bringing a heightened complexity to the CFD model.

4-stroke engine CFD simulations have become standard engineering applications thanks to the developing software infrastructure (Taylor et al., 2018; Aguerre et al., 2022). Simplified in-cylinder simulations can substantially provide the necessary information for combustion at 4-stroke engine simulations. This eliminates the need to model valve movements, thus helping to simplify the model. Some studies (Wang & Zhang, 2023) on two-stroke engines don't require valve movement since it is possible to simplify CFD models. However, the scavenging process generally need to include the dynamic CFD simulation to model gas flow and combustion at two-stroke engines. It is critical to correctly solve the scavenging process because it plays an essential role in cylinder flow patterns and the overall engine performance for two-stroke engines (Faruoli et al., 2021). Correctly solving the gas flow between the in-cylinder region and intake & exhaust ports has critical importance because the air-fuel mixture and the residual exhaust gas are sucking and scavenging between these volumes. Using a proper turbulence model and mesh structure (Rulli et al., 2021) directly affects the flow prediction and amount of the fuel-air mixture inlet and exhaust gas outlet between these volumes. The solution of these parameters provides the combustion prediction properly of the two-stroke engine.

Today, ICE continues to be widely used in many areas, such as transportation, energy, and agriculture. With the widespread use of ICE, the need for these engines has increased continuously. Simultaneously, continuous innovations have emerged for ICE to work more efficiently.

Combustion in ICE can be defined as the conversion of the energy released into work as a result of obtaining

optimum temperature and pressure conditions for the amount of air and fuel mixture in the combustion chamber. Today, during the engine development process, it is of great importance to examine the amount of mixture taken into the cylinder in these engines, fuel injection dynamics, ignitions, swirl ratio, heat transfer, the complex structure of the combustion process, and to determine the effects of all parameters that may affect engine performance (Johnson, 2009). However, examining the effects of parameters that will affect engine performance using experimental methods is a very difficult, costly and time-consuming process (Coskun et al., 2017, 2019).

For this reason, mathematical models have been developed to examine these effects, taking into account the disadvantages in experimental studies. When mathematical modeling is applied to ICE, it appears as a faster solution and a cost-saving method in experimental studies. Mathematical modeling technique offers us the opportunity to examine many parameters obtained from the engine model, depending on or independent of time. In this context, in light of this information, the computational fluid dynamics (CFD) method, a mathematical modeling technique, was developed and has become frequently preferred today. It is a branch of fluid mechanics that provides effective solutions and saves cost and time in the product development process as a result of modeling the realistic flow occurring in the ICE. The CFD method is based on the method of solving governing equations using numerical methods. It enables the solution of complex problems such as compressible, multi-phase, turbulent flow due to high Reynolds number at low Mach numbers, time-varying heat transfer and chemical reactions occurring in the combustion chamber (Abdulnaser, 2009).

Recently, the adaptive mesh refinement (AMR) strategy, an effective tool to simulate dynamic movements, has developed rapidly and adapted to CFD codes (Barros et al., 2022). The adaptive mesh strategy has brought significant convenience to the CFD world, providing an essential solution to issues arising from mesh errors, particularly in problems involving complex dynamics and motion (Lakhlifi et al., 2018; Coskun & Pehlivan, 2020; Demir et al., 2022b). Modeling two-stroke engines presents unique challenges due to their highly unsteady gas exchange processes, simultaneous intake and exhaust events, and intricate turbulence dynamics. These complexities make achieving accurate computational predictions difficult, particularly in terms of flow separation, scavenging efficiency, and combustion stability. Additionally, mesh dependency and turbulence model selection significantly influence the reliability of simulation results, necessitating a careful balance between computational cost and accuracy.

In this study, a two-stroke, two-cylinder gasoline engine was modeled using the Ansys Forte ICE simulation tool, and a validation study was conducted by comparing

Table 1 Engine specifications

Description	Specification
Engine Speed (RPM)	4800
Cylinder Bore [mm]	64
Stroke [mm]	64
Connecting Rod Length [mm]	122
Cylinder Volume [mm ³]	206
Number of Cylinder	2
Compression Ratio	9.4
Intake Opening	127 CAD
Intake Closing	233 CAD
Exhaust Opening	90 CAD
Exhaust Closing	270 CAD
Number of Spark (For single cylinder)	1
Cooling	Air Cooled
Fuel	Gasoline
Usage Area	Aviation

Table 2 The accuracy and sensitivity values of the experimental setup

Parameter	Measuring Device	Measuring Range	Accuracy	Uncertainty Value
Total mass flow rate	Air Flow Meter	0-780 [kg/h]	±0.5%	±3.9 kg/h
Fuel mass flow rate	Fuel Flow Meter	0-125 [kg/h]	±0.5%	±0.625kg/h
Torque	Torquemeter	0-500 [Nm]	±0.05%	±0.25 Nm
Indicated Power	Dynamometer	Calculated	±0.5%	±0.66kW
Indicated Specific Fuel Consumption (ISFC)	Derived from Mass Flow	Calculated	±1.0%	±3.5 g/kWh
Volumetric Efficiency	Derived from Air Flow	Calculated	±0.8%	±0.012

the numerical results with experimentally measured engine performance parameters. By systematically analyzing the impact of different turbulence models (Standard $k-\epsilon$ and RNG $k-\epsilon$) and mesh sizes (2 mm, 3 mm, and 4 mm), this study identifies the most suitable modeling approach for enhancing simulation fidelity and predictive accuracy. The findings provide valuable insights into optimizing CFD methodologies for two-stroke aviation engines and contribute to the ongoing efforts to improve computational modeling strategies for better engine design, performance evaluation, and fuel efficiency predictions.

2. MATERIALS AND METHOD

An experimental setup has been prepared for a 2-stroke aviation engine. Data were obtained for constant RPM and ambient conditions from the experimental studies. CFD simulations were done using 3D engine model. Two different turbulence model and three different mesh strategy were used.

The results obtained from the experimental data were compared with the simulation study, and the most appropriate simulation strategy was determined.

2.1 Experimental Procedure

Information about the 2-stroke engine used in experimental studies is given in Table 1. The experiments were carried out at a constant speed of 4800 rpm and at

full load. Data began to be collected after the air-cooled engine was thermally stabilized.

In the experimental study, AVL measuring equipment were used. The maximum capacity of the dynamometer was 132 kW. The accuracy and sensitivity values of the measurements made in the experimental study are shown in Table 2. The accuracy values were obtained from the AVL measuring equipment used in the experimental setup. The key measurement devices and their corresponding uncertainties are listed in the table provided. The accuracy of the total mass flow rate and fuel mass flow rate is ±0.5%, while the torque measurement accuracy is ±0.05%. Derived parameters, such as indicated power, indicated specific fuel consumption (ISFC), and volumetric efficiency, have estimated uncertainties of ±0.5%, ±1.0%, and ±0.8%, respectively. These uncertainty values demonstrate the precision of the experimental setup. The relatively low uncertainty in torque and power measurements suggests a high level of confidence in the performance parameters. However, derived parameters like ISFC have slightly higher uncertainty due to the propagation of errors from mass flow and power calculations. Based on the calculated uncertainty values, the total mass flow rate has an uncertainty of ±3.9 kg/h, while the fuel mass flow rate uncertainty is ±0.625 kg/h. Torque measurement uncertainty is ±0.25 Nm, and the indicated power uncertainty is ±0.66 kW. For the derived parameters, the ISFC uncertainty is ±3.5 g/kWh, and the volumetric efficiency uncertainty is ±0.012. These values indicate

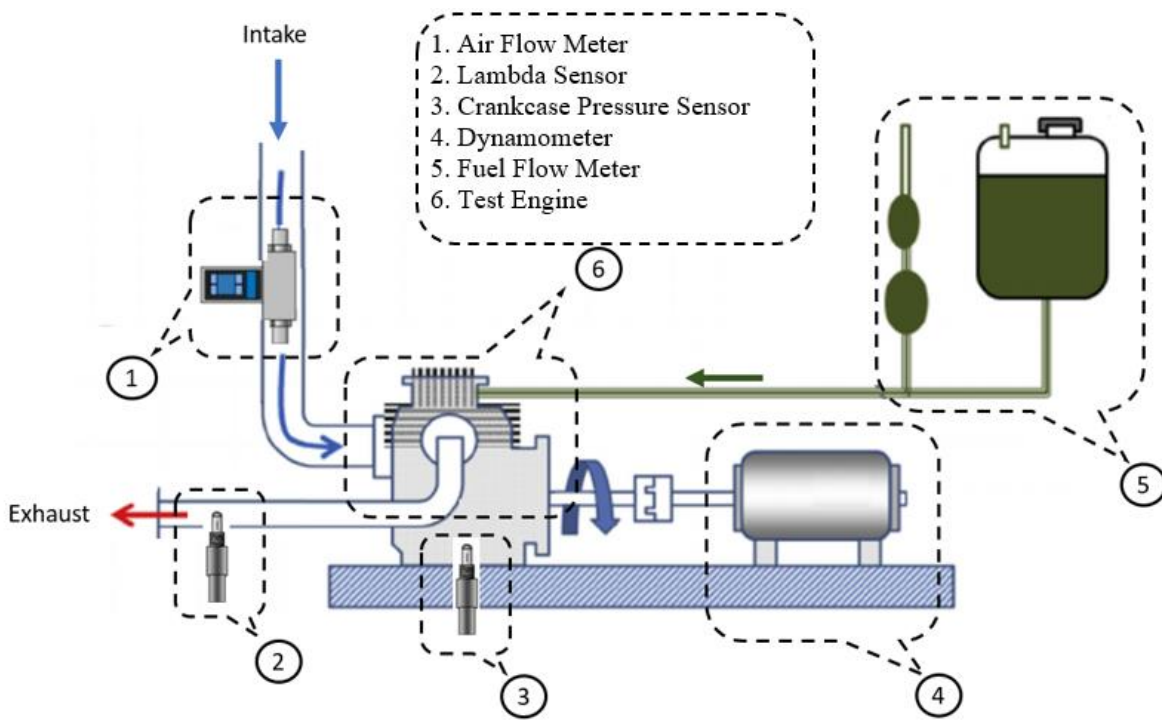


Fig. 1 Diagram of the test setup

that while the primary measurements have minimal uncertainty, propagated errors in calculated parameters should be considered when interpreting the results. To further reduce uncertainties, measurements were recorded only after reaching steady-state conditions, minimizing transient fluctuations.

The schematic of the experimental setup is given in Fig. 1. A two-stroke, two-cylinder engine was connected to the dynamometer with a coupling. Intake air flow rate was measured instantaneously with AVL brand ultrasonic flow meter. Aviation gasoline fuel, which is used in the aviation industry, was used in the experiments. Mass fuel flow to the engine was measured with the fuel flow meter. Port injection system used in experimental engine to prepare premixed mixture. Experiments were run for 0.9 lambda value. In addition, the crankcase pressure was measured with a pressure sensor. Air-fuel ratio data was obtained from the exhaust outlet with the lambda sensor. The data collected from the engine during the test period was transferred to the control screen where the data will be displayed instantly. Data were collected after a minimum one-minute waiting period when the engine reached steady state conditions. With these measurements, indicated engine power, indicated specific fuel consumption and volumetric efficiency were obtained.

2.2 CFD Simulation

In this study, a CFD simulation of a two-stroke and two-cylinder gasoline engine was performed using Ansys-Forte software. A comparison was made between the data obtained from the simulation in which a single cylinder was modeled and the experimental data.

For CFD analysis, it is first necessary to create the flow volume of the engine combustion chamber. Figure 2

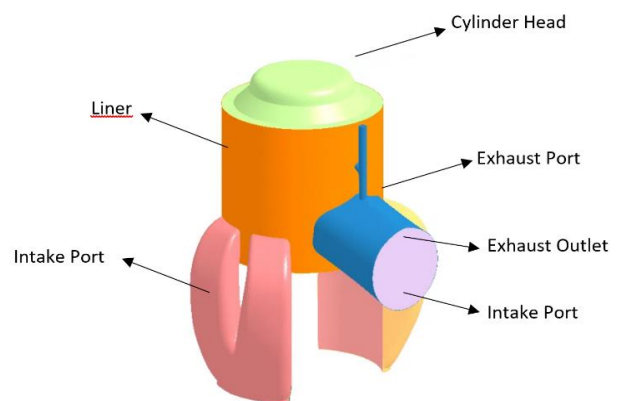


Fig. 2 CAD Model used at CFD simulation

shows the 3D solid model of the flow volume of the single cylinder of a two-stroke engine. 3D CAD model; two solid models (volumes) were created by dividing the flow volume into two parts: the flow volume (intake manifold, exhaust manifold, dead volume and cylinder head) and the volume swept by the piston. The most important factor in dividing it into two: flow volume and volume swept by the piston is to ensure that the dynamic mesh model of the piston is run automatically by the software. In addition, a by pass design was used in the CFD model. This is because with the temperature and pressure increases in the cylinder caused by combustion, a very high speed occurs as soon as the exhaust starts to open. In order to prevent high speeds occurring here, a by-pass design is created to prevent excessive acceleration. After the 3D model was created, surface names were made and boundary conditions were determined in the simulation program. In boundary conditions, 573 K was defined as the constant temperature of the upper part of the combustion chamber

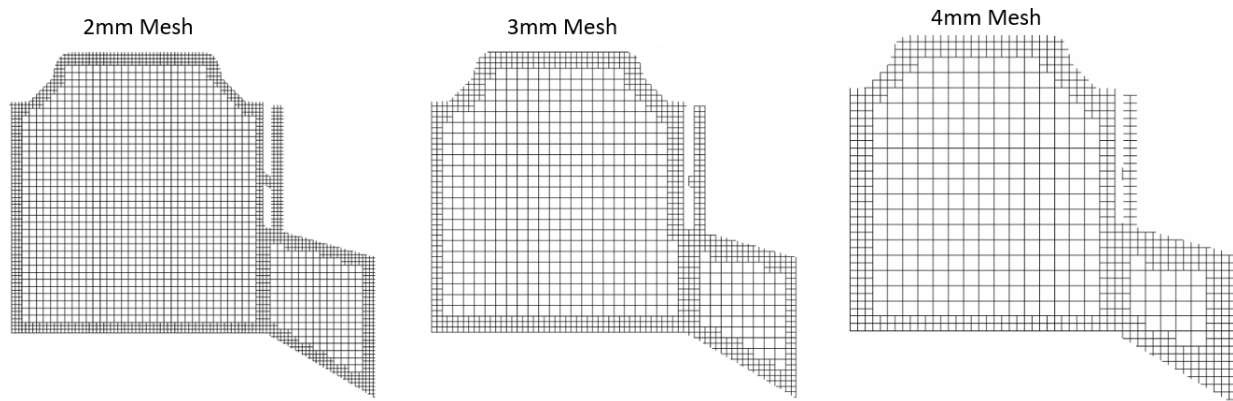


Fig. 3 Mesh view according to different mesh sizes at 180 CAD

Table 3 Turbulence models, mesh size and computational cost

Turbulence Model	Mesh Size [mm]	Total wall-clock time	Total CPU time
RNG k- ϵ	4	5 h, 46 min	5 d, 13 h
RNG k- ϵ	3	4 h, 35 min	4 d, 9 h
RNG k- ϵ	2	9 h, 2 min	10 d, 4 h
Standard k- ϵ	4	6 h, 7 min	5 d, 20 h
Standard k- ϵ	3	4 h, 48 min	4 d, 14 h
Standard k- ϵ	2	9 h, 0 min	8 d, 15 h

and the liner. The intake port is defined as 300 K constant temperature. The exhaust port is defined to have a constant temperature of 490 K. Convective wall heat transfer flux is modeled for given wall temperature, by using the Han-Reitz Model. For the wall slip conditions “Law of the Wall” model used for simulations. For all wall conditions, the roughness height was set to 1 micron, while the roughness constant was defined as 0.5 in the model. Default Wall Function is chosen for wall shear model. RNG k- ϵ (Han & Reitz, 1995) and Standard k- ϵ (Lauder et al., 1973) turbulence models were used for CFD simulation.

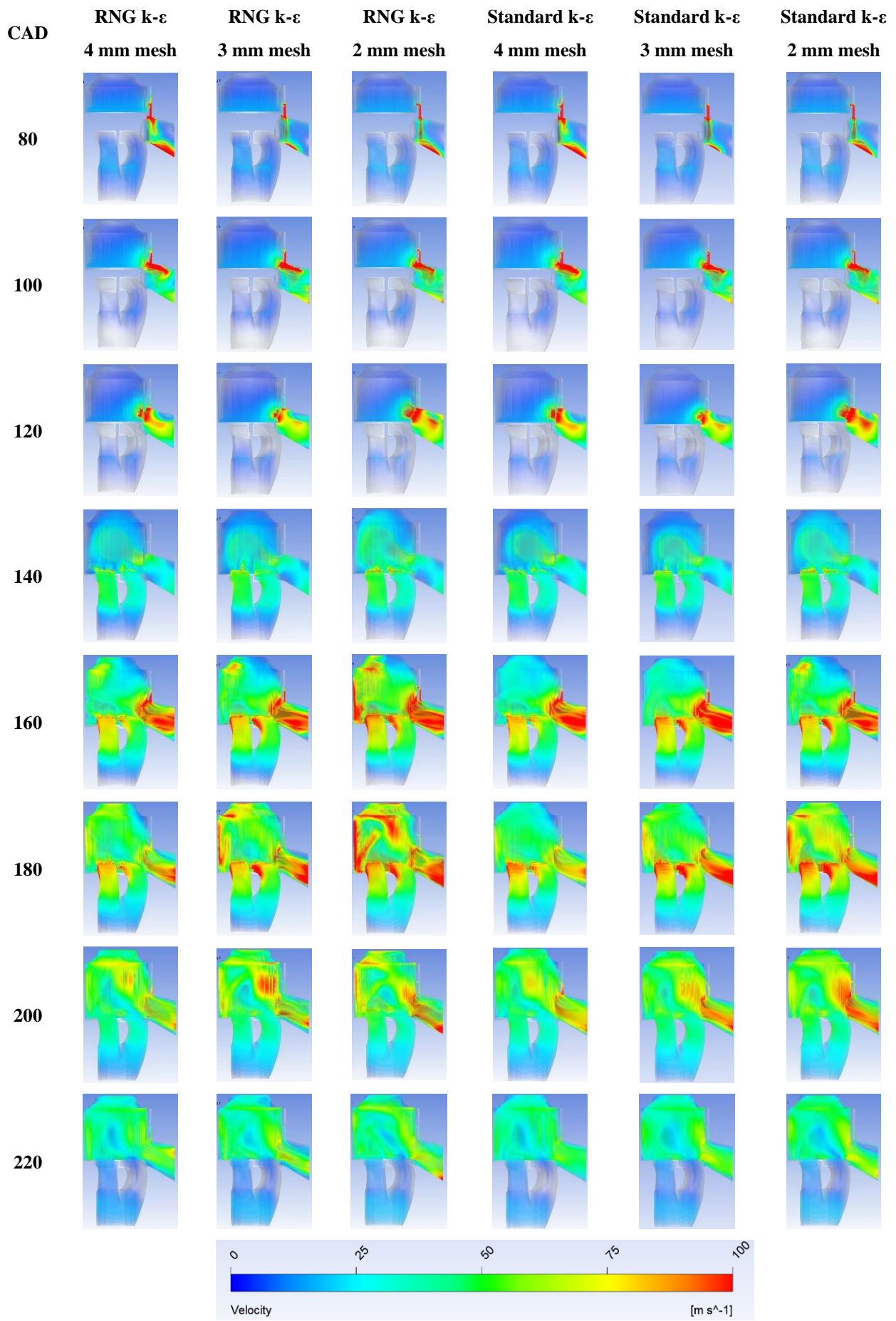
Since aviation gasoline was used in the experiment, it is known that this fuel has an octane number of 100. iC_8H_{18} fuel was used to simulate the combustion of this fuel. There are a total of 59 species and 436 reactions (Li et al., 2019) in the chemical kinetic mechanism used in the simulation study and included in the Forte software, including the soot and extended Zeldovic NO_x model. A spark model was used to simulate the spark ignition of a two-stroke, two-cylinder spark ignition engine. The energy release value in the spark model was used as 32 j/sec. The internal kernel radius value was defined as 0.1 mm. Spark ignition is defined in the model as in the experimental engine, starting from 340 CAD and continuing a total of 48 CAD, in other words spark runs from 20 deg bTDC to 28 deg aTDC. The simulation was run in the range of 60-420 CAD which includes bypass time. For the time-dependent solution, the software automatically determined the step interval by setting it to a maximum of $1.0E-5$ s.

Experimentally obtained inlet fuel, air, and time depended inlet pressure as pressure profile data entered to the CFD model as inlet condition. For inlet temperature

isentropic condition which automatically calculates inlet temperature according to isentropic behavior used for the CFD model. Additionally, the experimentally measured crankcase pressure profile was used to define the intake port time-dependent pressure boundary condition.

Since Ansys-Forte uses automatic mesh generation (AMG) and AMR strategies for mesh structure, these methods were used for current simulations. Within the scope of the analysis, solutions were made in 2mm, 3mm and 4mm global mesh sizes, and the results obtained from the experimental data and results were compared with simulations. The global mesh size of all surfaces was reduced by $\frac{1}{4}$ throughout the entire simulation process, thus providing a more accurate resolution of near wall calculations. Additionally, the global mesh size was reduced by $\frac{1}{8}$ during the spark moment in the spark region. The mesh size was reduced by $\frac{1}{2}$ between 274-420 CAD, which is the period in combustion. The global mesh size of the exhaust and intake port surfaces was reduced by $\frac{1}{2}$ during the intake and exhaust time interval. Mesh images of 180 CAD angles are given in Fig. 3.

As the mesh size decreases, the solution time is naturally expected to increase. However, due to the automatic mesh size control implemented by the adaptive mesh strategy, unexpected variations in solution time may sometimes occur. As shown in Table 3, the total simulation time varies for different mesh sizes and turbulence models. The general trend indicates that a smaller mesh size leads to longer solution times. However, for 3 mm and 4 mm mesh sizes, deviations from this trend are observed due to the effects of the adaptive mesh strategy. It is found that the simulation performed with a 3 mm mesh size is 21% shorter than that with a 4 mm mesh size for both turbulence models.



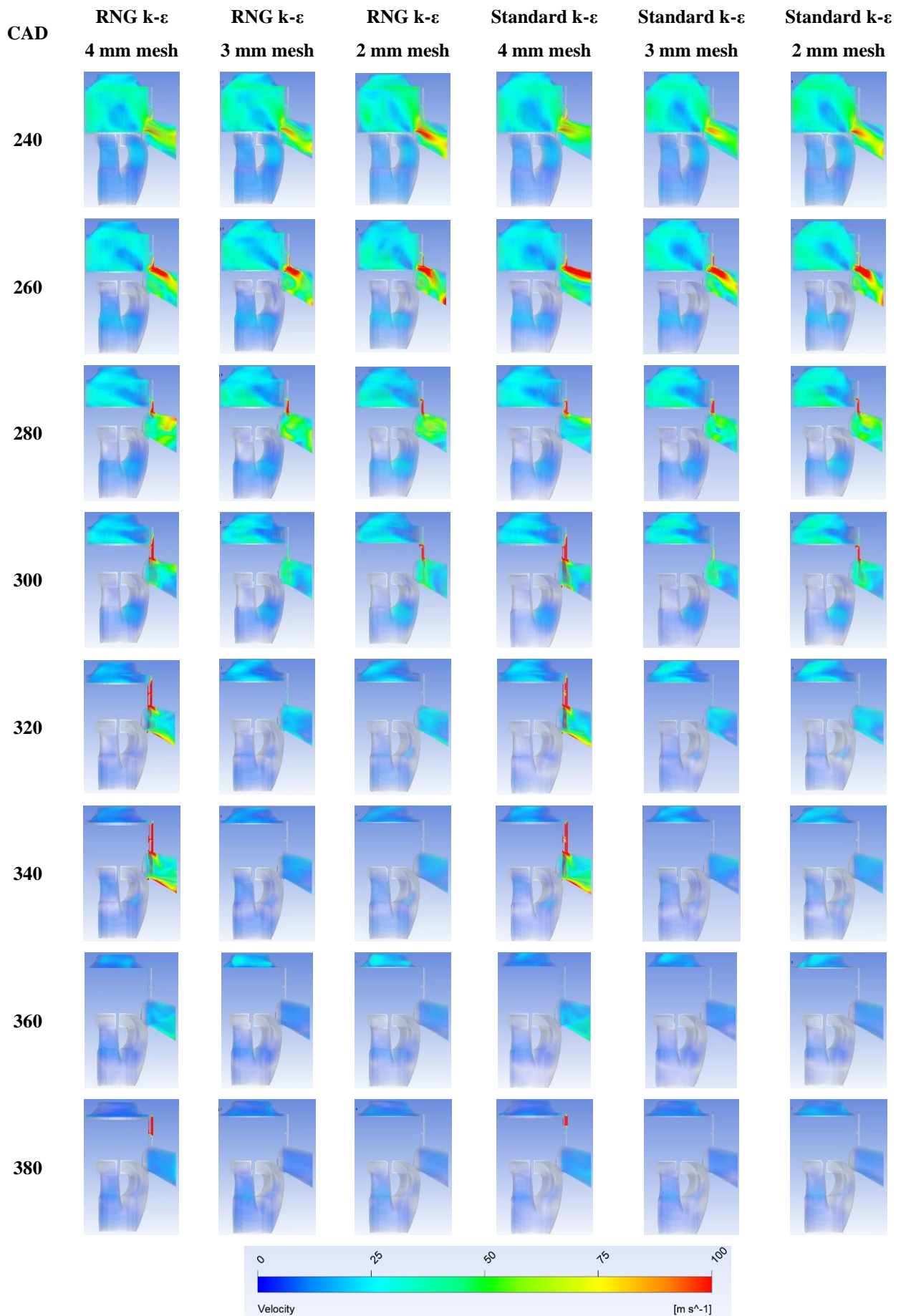


Fig. 4 Velocity distribution for RNG and Standard $k-\epsilon$ models with 4, 3, and 2 mm mesh sizes

3. RESULTS

Within the scope of the analysis, a comparison was made between 2, 3, and 4 mm mesh sizes and two different turbulence models as Standard $k-\epsilon$ and RNG $k-\epsilon$.

Figure 4 presents the in-cylinder velocity distributions obtained from the CFD simulations, captured at every 20 CAD from 80 CAD to 380 CAD. The analysis reveals significant variations in flow behavior based on turbulence models and mesh sizes, influencing the accuracy of the results. At 80 CAD, the bypass port opens, resulting in high-velocity gradients in this region. When the exhaust port opens at 100 CAD, velocity variations occur in both the bypass valve and exhaust port areas, illustrating the complex interaction of intake and exhaust flows. Between 160-180 CAD, the in-cylinder velocity intensifies as the piston approaches bottom dead center (BDC), where both the intake and exhaust ports are fully open. These regions exhibit strong turbulence, particularly in the simulations utilizing finer mesh resolutions (2 mm and 3 mm). As the ports close sequentially—intake at 233 CAD, exhaust at 270 CAD, and bypass at 320 CAD—a gradual reduction in velocity is observed within the cylinder. From 380 CAD onwards, simulations with a 4 mm mesh size and the RNG $k-\epsilon$ model exhibit significant velocity discrepancies compared to other cases. This discrepancy arises due to flow leakage at the exhaust port, a result of an insufficiently refined mesh, which fails to accurately capture small-scale turbulence structures. This effect highlights the need for finer meshing in critical regions to reduce numerical dissipation and better represent flow physics. In the low-velocity regions, there is no significant difference between the RNG $k-\epsilon$ and Standard $k-\epsilon$ models across all mesh sizes. However, distinct differences emerge at 160, 180, and 200 CAD, where the flow rate increases sharply throughout the cylinder volume. This trend is particularly pronounced in the 3 mm and 4 mm mesh cases, where the RNG $k-\epsilon$ model predicts steeper velocity gradients compared to the Standard $k-\epsilon$ model. These observations suggest that the RNG $k-\epsilon$ model provides a more refined resolution of turbulent kinetic energy dissipation, potentially leading to improved accuracy in predicting flow structures critical to combustion and scavenging efficiency. These observations suggest that the RNG $k-\epsilon$ model provides a more refined resolution of turbulent kinetic energy dissipation, potentially leading to improved accuracy in predicting flow structures critical to combustion and scavenging efficiency.

At 220 CAD and beyond, the differences between turbulence models diminish as the velocity gradients stabilize across the chamber. However, at 300, 320, and 340 CAD, significant differences appear in the bypass region, particularly in simulations with larger mesh sizes. In the 4 mm mesh case, the bypass line does not close properly, leading to persistent velocity gradients, whereas simulations using a 2 mm mesh effectively capture bypass closure at 320 and 340 CAD. These results emphasize the importance of mesh refinement in regions of rapid flow transitions. The RNG $k-\epsilon$ model's superior resolution of turbulent structures, particularly at high-flow-rate CADs, results in better predictions of velocity gradients compared

to the Standard $k-\epsilon$ model. This behavior is crucial when analyzing engine performance metrics such as specific fuel consumption, as turbulence directly affects the fuel-air mixing process. The observed improvement in specific fuel consumption predictions using the RNG $k-\epsilon$ suggests that this model is better suited for applications where turbulence-driven mixing efficiency plays a significant role in performance and emissions. Thus, the choice of turbulence model and mesh size has a direct impact on the fidelity of CFD simulations. While coarser meshes (4 mm) lead to leakage issues and inaccurately resolved flow gradients, finer meshes (2 mm) provide a more detailed representation of critical flow features, particularly in bypass and exhaust port regions. These findings reinforce the necessity of carefully selecting numerical parameters to ensure robust and physically meaningful simulations in two-stroke engine modeling.

Figure 5 shows the temperature distribution in the combustion chamber for different mesh sizes and turbulence models between 260-420 CAD. The intake port closes at 233 CAD, the exhaust port at 270 CAD, and the bypass port at 320 CAD. During this period, the temperature inside the combustion chamber increases gradually as compression progresses.

For both turbulence models, the overall temperature distribution is similar, but small variations appear depending on mesh size. These differences become more noticeable after 344 CAD, when ignition starts to affect the temperature distribution. At 340 CAD, the temperature of the compressed air-fuel mixture begins to rise sharply due to ignition. The peak in-cylinder temperature reaches about 2540 K at 372 CAD, and after this point, the temperature starts to decrease gradually until 420 CAD as the expansion process takes place.

Up to 372 CAD, the temperature gradient patterns remain consistent across different mesh sizes, except for some variations that begin at 344 CAD, where the effects of ignition become more visible. At this moment, it is observed that larger mesh sizes lead to a wider distribution of high-temperature regions. This is a common behavior in CFD simulations, where coarse meshes can negatively impact temperature calculations due to numerical dissipation. Therefore, using refined meshes and inflation layers in boundary regions is essential for more accurate thermal predictions.

At 344 CAD, a key difference between turbulence models emerges:

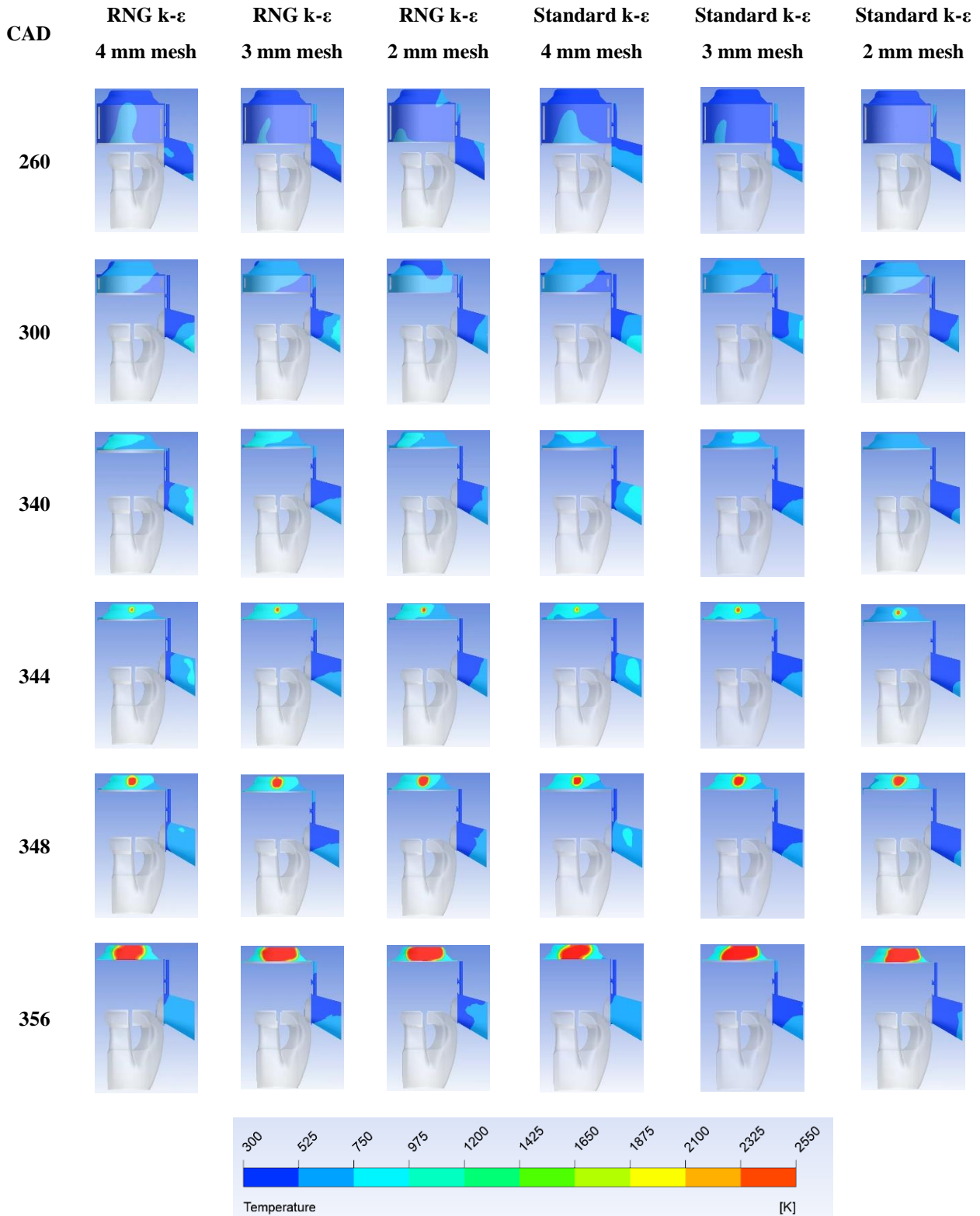
- The Standard $k-\epsilon$ model predicts larger cold regions compared to the RNG $k-\epsilon$ model.
- This suggests that the Standard $k-\epsilon$ model better captures localized cooling effects, providing more precise temperature distribution in these areas.
- This trend continues in later CADs, reinforcing the impact of turbulence models on combustion temperature predictions.

Between 390-412 CAD, differences in temperature gradients due to mesh size become more pronounced. While both turbulence models produce similar in-cylinder temperature distributions, variations in mesh structure

cause temperature differences in the bypass valve and exhaust port regions. This indicates that mesh refinement is important for accurately capturing post-combustion heat transfer effects.

Overall, the results show that in the RNG $k-\epsilon$ model, reducing the mesh size causes the high-temperature

regions to expand. This happens because the RNG $k-\epsilon$ model provides better resolution of small-scale turbulence structures, leading to more accurate predictions of temperature gradients. The improved ability of this model to capture flame propagation and post-ignition heat distribution makes it more suitable for simulating turbulent combustion processes with higher accuracy.



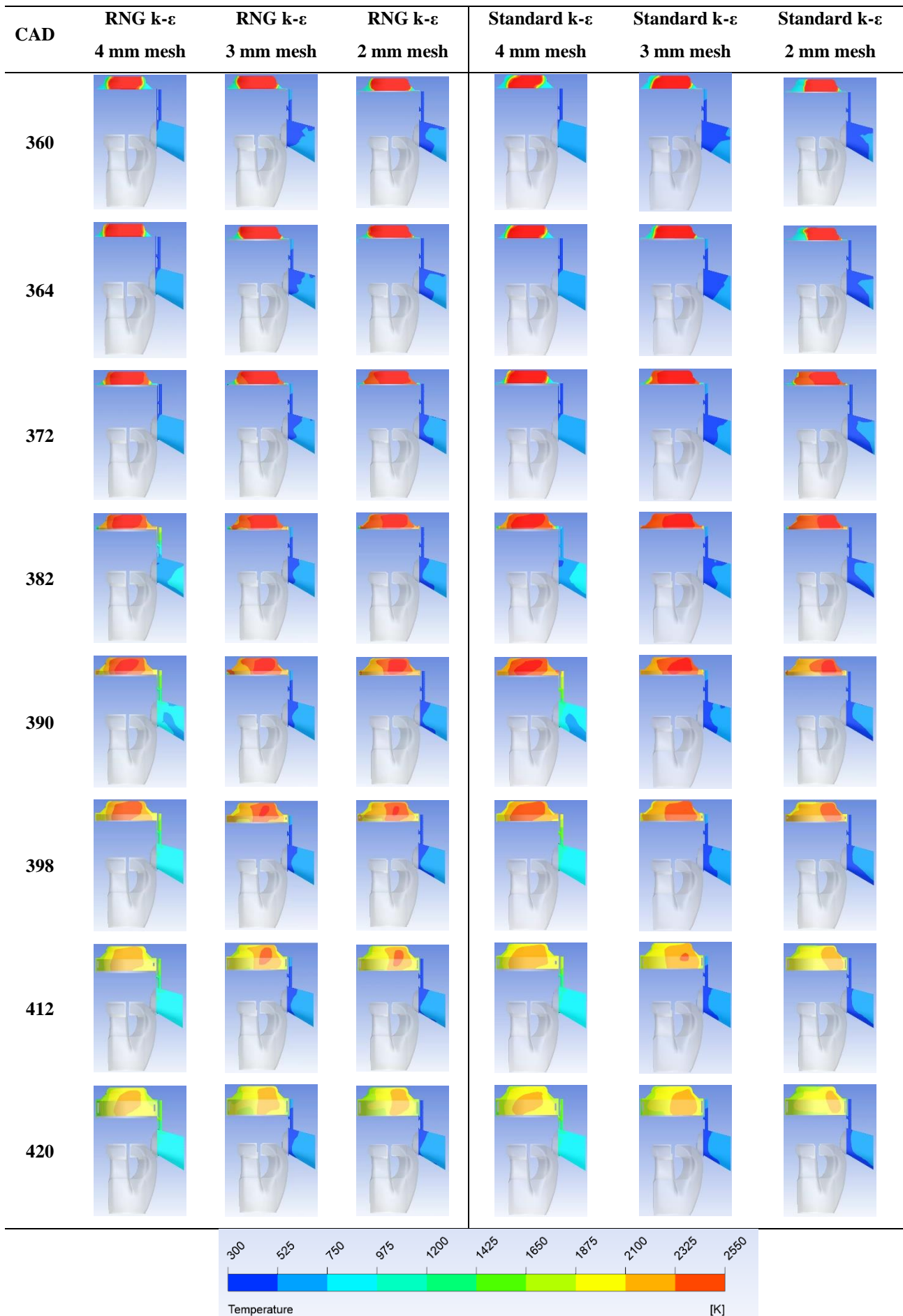


Fig. 5 Temperature distribution for RNG and Standard k- ϵ models with 4, 3, and 2 mm mesh sizes

These findings confirm that choosing the right turbulence model and mesh size is crucial in CFD studies of two-stroke engines. The accuracy of combustion characteristics, thermal distribution, and overall engine performance predictions depend heavily on these factors

3.1 Comparison of Experimental and Simulation Results

This section compares and evaluates the data obtained from the experimental engine and the simulation results solved by the CFD method.

Figure 6 shows the test and simulation results obtained at a constant engine speed of 4800 rpm. Total mass flow rate, fuel mass flow rate, volumetric efficiency, indicated engine power and indicated specific fuel consumption were measured experimentally and obtained from simulations to compare. The error rates presented in the figures were calculated by comparing the data obtained from each simulation with the experimentally obtained data. All error rates individually indicate the discrepancies between the CFD calculations and the experimental data.

The total mass flow rate was experimentally measured as 145 kg/h. It is seen that the simulation results are getting closer to the experimental data by decreasing the mesh size in both the RNG and the standard $k-\epsilon$ model. The simulation using the Standard $k-\epsilon$ turbulence model with 2mm mesh size results of 131,9 kg/h is the closest result to the experimental data. The lowest value was obtained with the RNG $k-\epsilon$ turbulence model with a mesh size of 4 mm. The experimental result closest to the simulation based on error rate is 9%. The worst convergence is obtained from 4 mm mesh size RNG $k-\epsilon$ turbulence model, with an error rate of 18%.

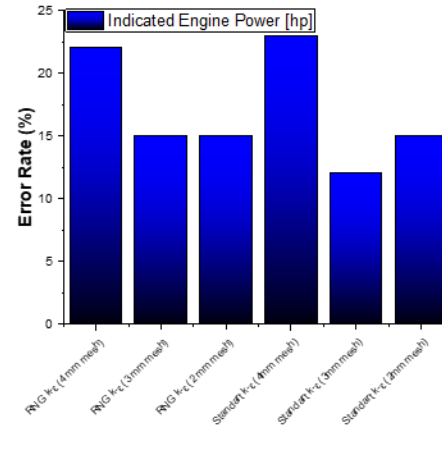
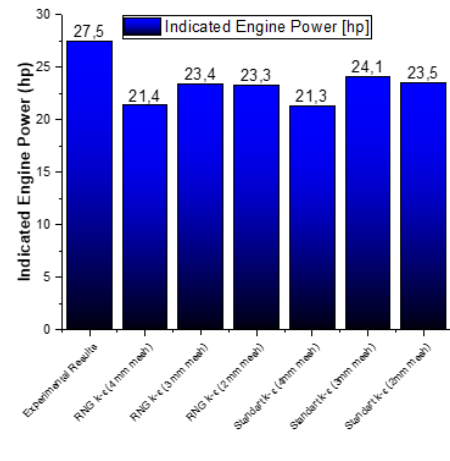
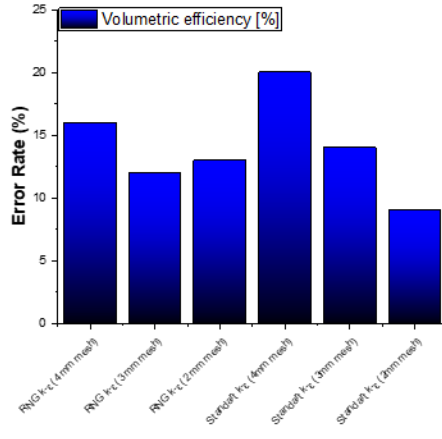
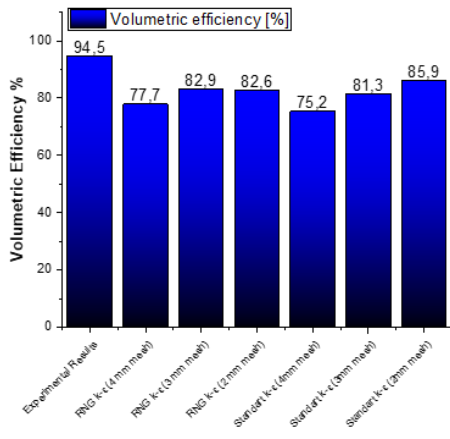
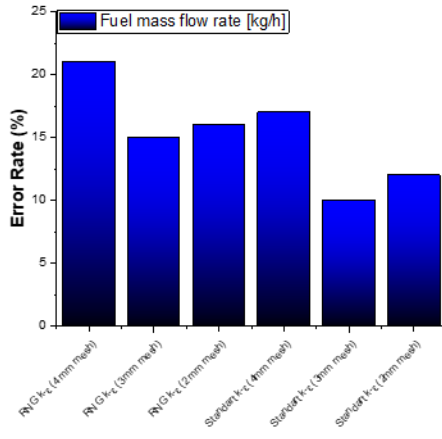
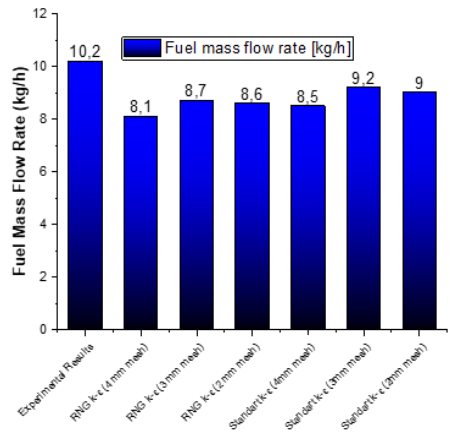
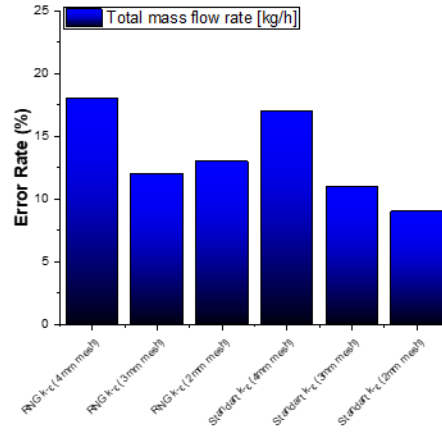
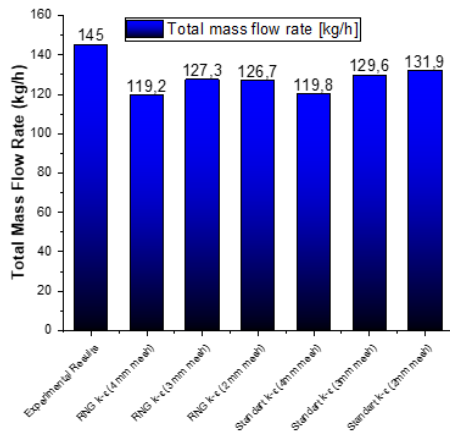
While the fuel mass flow rate was experimentally measured as 10.2 kg/h, the lowest value of 8.1 kg/h was obtained in the simulations at the RNG $k-\epsilon$ turbulence model with the 4 mm mesh size, and the highest value of 9.2 kg/h was obtained in the simulations at the standard $k-\epsilon$ turbulence model with the 3 mm mesh size. In other words, it was concluded that the standard $k-\epsilon$ turbulence model with 3 mm mesh size, in which the best convergence was achieved, had a 10% error rate, while the 4 mm mesh size RNG $k-\epsilon$ turbulence model, in which the furthest convergence was achieved, had a 21% error rate.

Theoretically, the mass gas flow rate that can be fed to the engine is calculated as 153.5 kg/h; at this value, the volumetric efficiency in the engine is 100%. In the experimental study, the mass gas flow rate was measured as 145.5 kg/h, and the volumetric efficiency was calculated to be 94.5%. The closest value to the test result for volumetric efficiency was obtained as 85.9% from the standard $k-\epsilon$ simulation with 2 mm mesh size, and the error rate was calculated as 9%. The worst value of the volumetric efficiency was 75.2% obtained from the standard $k-\epsilon$ simulation with 4 mm mesh size, and the error rate was calculated as 20%. Since the total mass flow rate analysis results are lower than the experimental results, the volumetric efficiency is also low.

In the experimental study, the indicated engine power was measured as 27.5 hp. As a result of the analysis, the lowest indicated engine power was calculated as 21.3 hp for the standard $k-\epsilon$ turbulence model with 4 mm mesh size. The biggest indicated engine power was calculated as 24.1 hp for the standard $k-\epsilon$ turbulence model with 3 mm mesh size. The indicated engine power closest to the experimental result was obtained from the standard $k-\epsilon$ simulation with 3 mm mesh size with a 12% error rate. The average of all analysis results in other turbulence model and mesh sizes was calculated as 23.4 hp. The highest accuracy rate for fuel mass flow rate was calculated as 90%. According to the simulation, the indicated engine power was lower than the experimental results because the fuel mass flow rate was lower than the experimental results.

The experimental results indicated that specific fuel consumption was measured as 504 g / kWh. According to the simulation results, the lowest specific fuel consumption was calculated as 503.5 g/kWh for the RNG $k-\epsilon$ turbulence model and 3 mm mesh size, while the highest was calculated as 540.5 g/kWh for the standard $k-\epsilon$ turbulence model and 4 mm mesh size. The closest value to the experimental result for specific fuel consumption was obtained at 3 mm and 2 mm mesh sizes of the RNG $k-\epsilon$ turbulence model. According to the simulation results for specific fuel consumption, the lowest error rate was 0.1% at RNG $k-\epsilon$ 2 mm mesh size. In the results for specific fuel consumption, the data obtained in the RNG $k-\epsilon$ turbulence model converged more to the experimental result than the values obtained in the standard $k-\epsilon$ turbulence model. In the simulations, a decrease in the indicated specific fuel consumption was observed due to the total mass flow rate compared to the experimental results.

The thermal efficiency values obtained from both experimental measurements and CFD simulations using different turbulence models and mesh sizes are compared. The experimental thermal efficiency was measured as 16.23%, serving as the benchmark for evaluating simulation accuracy. From the simulation results, the RNG $k-\epsilon$ turbulence model with a 3 mm mesh achieved the closest agreement with experimental data, yielding a thermal efficiency of 16.19%. Similarly, the RNG $k-\epsilon$ model with a 2 mm mesh resulted in 16.30%, further validating the effectiveness of this turbulence model in predicting combustion characteristics. In contrast, the Standard $k-\epsilon$ model exhibited lower thermal efficiency values across different mesh sizes. The lowest efficiency was 15.08% for the Standard $k-\epsilon$ with a 4 mm mesh, indicating higher energy losses or inaccuracies in combustion and heat transfer predictions when coarser mesh resolutions were used. The results suggest a significant impact of mesh size on simulation accuracy. As the mesh was refined from 4 mm to 2 mm, the thermal efficiency predictions improved across both turbulence models. This indicates that finer mesh sizes provide better resolution of in-cylinder flow structures and combustion dynamics, leading to more accurate thermal efficiency predictions.



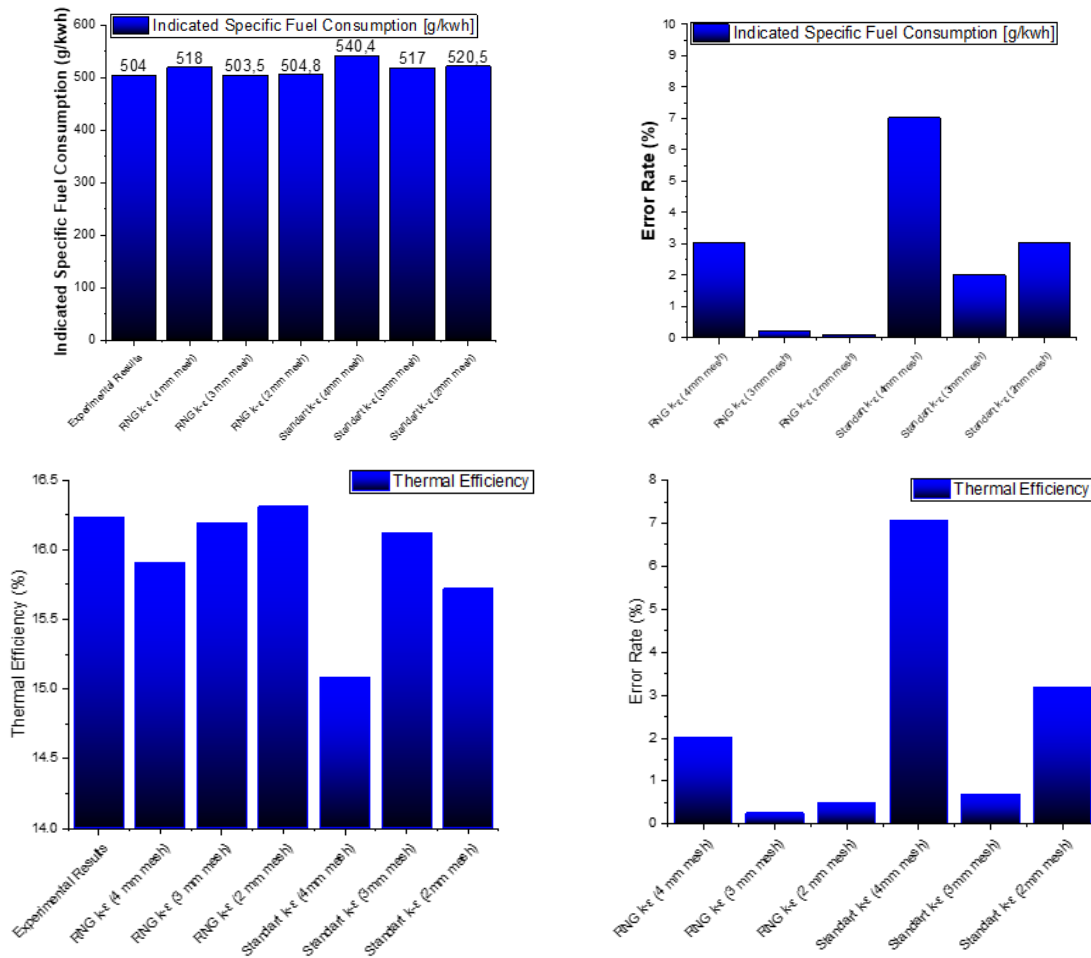


Fig. 6 Comparison of experimental results with simulation results and error rates

However, despite this improvement, the Standard $k-\epsilon$ model consistently yielded lower thermal efficiencies compared to the RNG $k-\epsilon$ model. This suggests that the RNG $k-\epsilon$ model better captures turbulent kinetic energy dissipation, which plays a crucial role in air-fuel mixing and combustion efficiency. The error rates between the experimental thermal efficiency (16.23%) and the simulated values were calculated. The RNG $k-\epsilon$ with 3 mm mesh had the lowest error rate (0.25%), while the Standard $k-\epsilon$ with 4 mm mesh had the highest error rate (7.07%). These findings indicate that the RNG $k-\epsilon$ model is more suitable for accurately predicting the combustion characteristics of two-stroke aviation engines.

Figure 7 shows the change of in-cylinder temperature depending on crank angle. Temperature data was not measured directly experimentally but was considered an indicator and evaluated for different turbulence models and mesh sizes. Since the engine is two-stroke, the intake and compression cycles occur simultaneously. There was a decrease in the in-cylinder temperature due to the warmer in-cylinder mixture during the intake period and the fresh charge being taken into the combustion chamber at a lower temperature from intake port. It is understood that the compression period fully begins around 200-225 CAD as a result of completing the intake process by blocking the front of the intake manifold with the upward movement of the piston. It can be said that combustion

begin almost simultaneously for all simulations and around 350 CAD. It is understood that the in-cylinder temperature varies significantly between 363 CAD, when the maximum temperature inside the cylinder is reached, and 388 CAD, when the temperature drops, at a global mesh size of 4 mm.

Figure 8 shows the maximum in-cylinder temperature values and the CAD in which these values occur. Findings are presented that allow understanding the effects of two different turbulence models (RNG $k-\epsilon$ and Standard $k-\epsilon$) used in CFD simulations on the solution at different mesh sizes. At a mesh size of 4 mm, convergence problems occur due to less data being received due to the lower number of meshes and the inability to fill some critical areas in sufficient quantities; it is understood that the simulation didn't work well at this mesh size. A similar trend was observed in both turbulence models, and as the mesh size decreased, the maximum in-cylinder temperature increased. This is because with smaller mesh sizes, the energy released by the chemical reaction was calculated more accurately, and the gradients near the combustion zone could be resolved more precisely. At 2 mm mesh size, temperatures obtained from the Standard $k-\epsilon$ model are slightly higher than the RNG $k-\epsilon$ model. This situation is probably because the Standard $k-\epsilon$ model is more sensitive to mesh improvement in the tested range or that turbulence slightly affects the combustion and heat

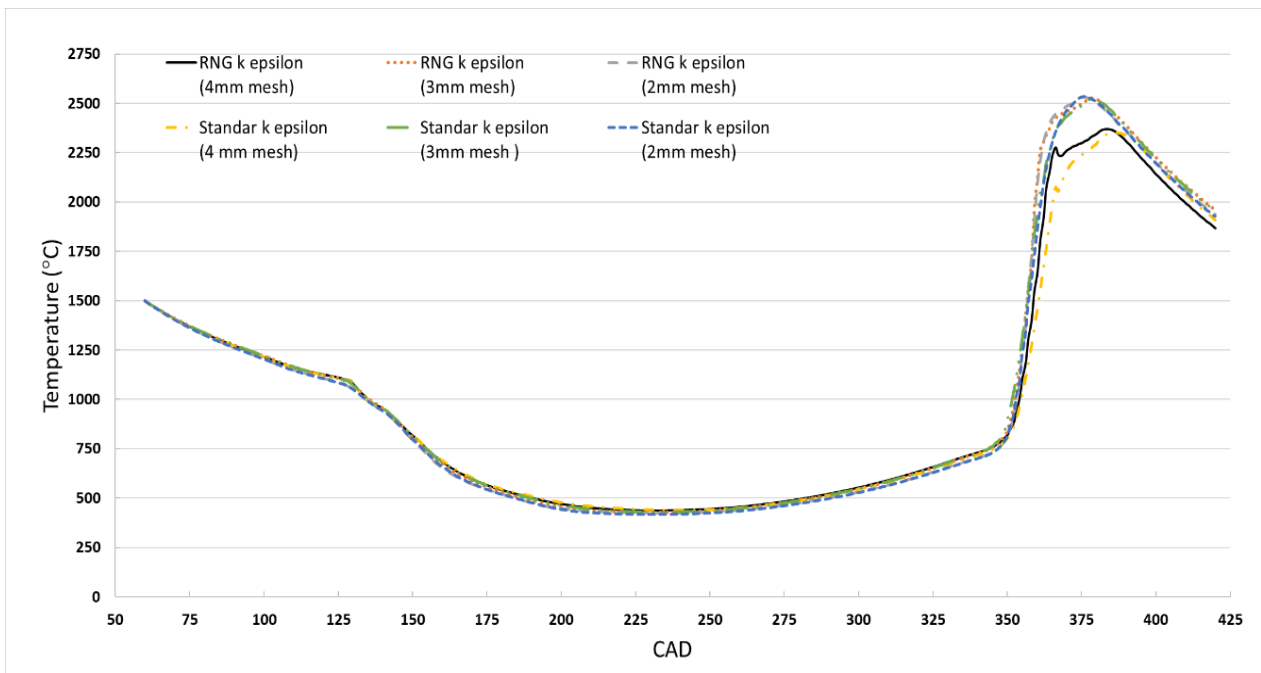


Fig. 7 Simulation results of in-cylinder temperature depending on crank angle

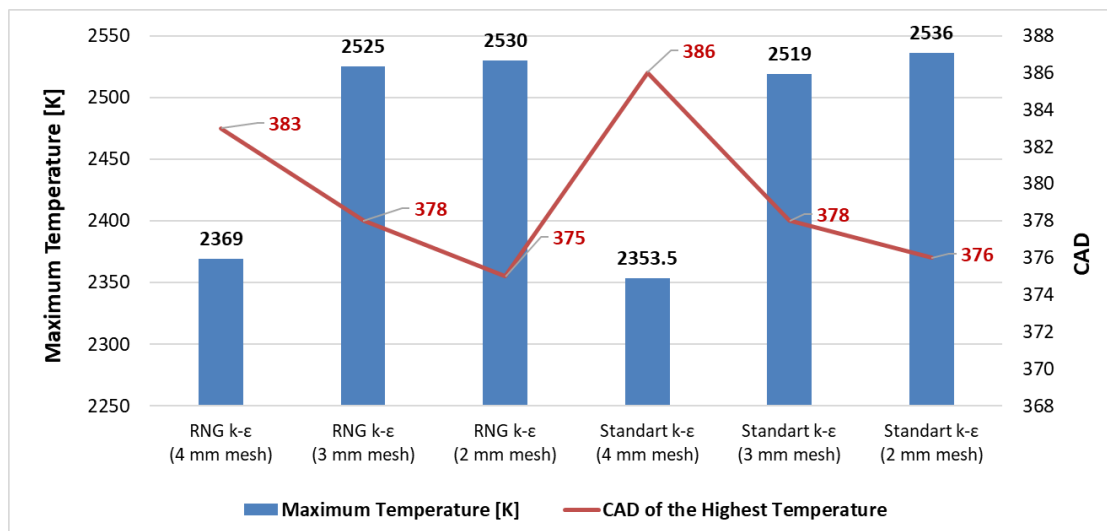


Fig. 8 Simulation results of maximum in-cylinder temperature and the CADs in which this value obtained

transfer solution and provides a higher temperature estimate. Simulations highlight the importance of mesh sensitivity analysis and show that smaller mesh sizes significantly affect the results.

The differences between the two turbulence models indicate that their suitability may vary depending on the particular engine design and operating conditions. Additional simulations with different engine configurations can help select the most suitable model. Comparing these simulation results with experimental data is important to verify the prediction accuracy of the models and their configurations. Variation in ignition timing is an important parameter in engine design and can affect the combustion performance and optimum combustion point of a two-stroke engine. Based on the findings, especially at small mesh sizes, changes in

ignition timing may be necessary to optimize performance. As a result, given in Fig. 8, it was understood that both turbulence models were sensitive to mesh size, and a slightly higher temperature was obtained from the Standard k-ε model with a global mesh size of 2 mm compared to other simulations. The CAD values at which the highest temperatures obtained from different mesh sizes show that the two turbulence models slightly affect combustion. Although the CAD values at which the maximum temperature values were obtained for the 3 mm mesh size were the same, there was a difference of 3 and 1 CAD for the 4 and 2 mm mesh sizes, respectively.

Figure 9 shows the in-cylinder pressure and heat release rate (HRR) change depending on the crank angle of simulations with different turbulence models and mesh sizes. It can be stated that similar results were obtained for

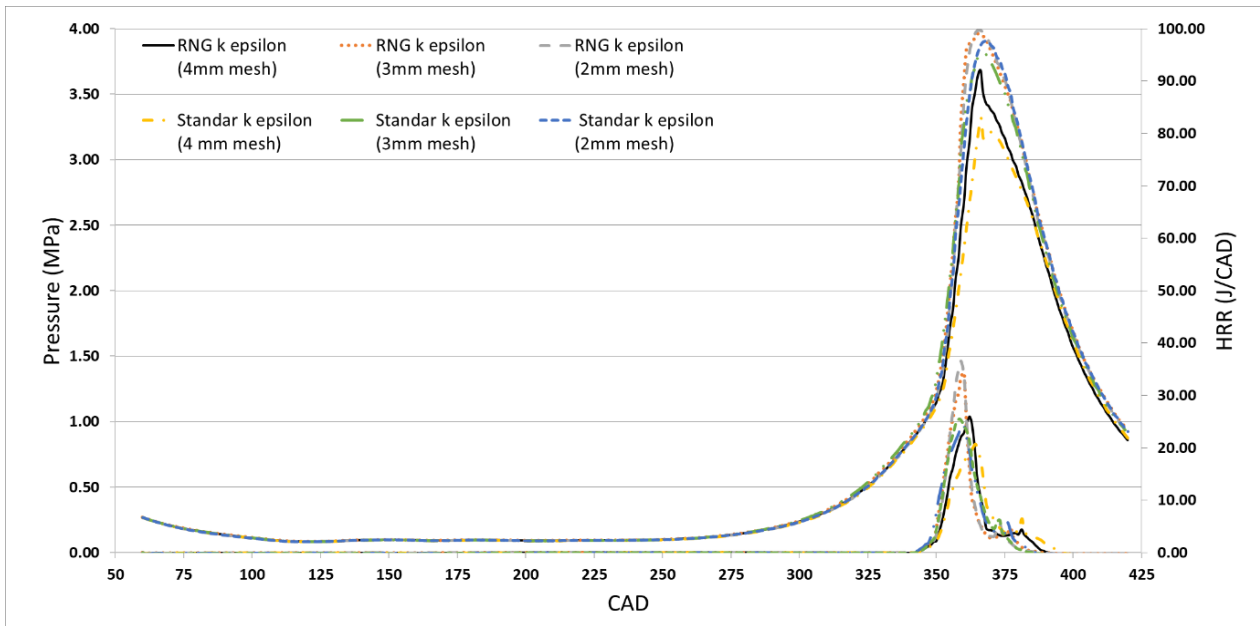


Fig. 9 Simulation results of in-cylinder pressure and HRR depending on crank angle

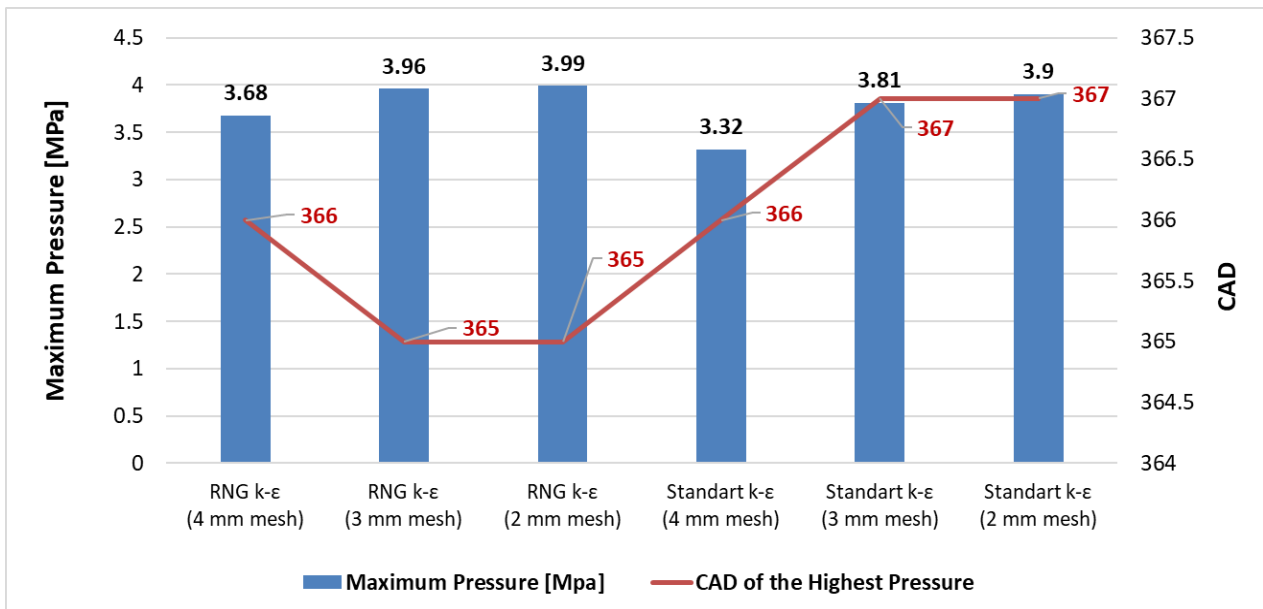


Fig. 10 Simulation results of maximum in-cylinder pressure and the CADs in which this value obtained

the pressure change depending on the crank angle in the intake and compression strokes, according to both turbulence models and three different mesh sizes. With the start of the combustion stroke, the pressure changes in the cylinder showed differences. Especially in the simulation results where the mesh size was 4 mm in both turbulence models, there was a difference in maximum pressure compared to other mesh sizes. It has been observed that simulations made with 3 and 2 mm mesh sizes give more consistent results. It is understood that at a mesh size of 4 mm, the maximum pressure is calculated with a deviation of more than 10%. In addition, it is seen that the turbulence model is effective in shifting the maximum pressure timing from top dead center. The same evaluations can be made for HRR data.

Figure 10 shows the maximum value of the in-cylinder pressure and the variation of the crank angle at which this value occurs according to different turbulence models and

mesh size. As the mesh size decreased from 4 mm to 2 mm, an increase in maximum in-cylinder pressure was observed for the RNG and Standard k-ε models. Maximum pressure increases with decreasing mesh size is generally observed in CFD simulations of ICE. As the mesh size decreased from 4 mm to 2 mm, the maximum in-cylinder pressure value increased for both RNG and Standard k-ε models. It can be said that a smaller mesh size typically allows for more accurate prediction of flow fields, reactions, heat transfer, and peak pressure in the simulation environment.

Higher and earlier in-cylinder pressures were obtained from the RNG k-ε for 3 mm and 2 mm mesh sizes compared to the Standard k-ε model. This suggests that the RNG k-ε model with additional damping functions may be more sensitive to obtain the maximum pressure inside the engine cylinder. The crank angle at which maximum pressure was observed did not vary

significantly between different mesh sizes for both models. It shows that the timing of maximum in-cylinder pressure is not significantly affected by the mesh size within the studied range. In both turbulence models, it was observed that the maximum pressure occurred at almost the same crank angle for 3 mm and 2 mm mesh sizes. However, the Standard k- ϵ model predicted the crank angle at which maximum in-cylinder pressure occurs slightly later than the RNG k- ϵ model.

4. CONCLUSION

In this study, flow and combustion simulation of a two-cylinder done using the CFD method by validating experimental results. The main purpose of the analysis studies was to examine the effect of mesh size and turbulence models in two-stroke engine CFD simulations. Total mass flow rate, fuel mass flow rate, volumetric efficiency, indicated engine power and indicated specific fuel consumption obtained at different turbulence and mesh sizes at 4800 rpm engine speed were compared with experimental results. Additionally, temperature and pressure changes in the cylinder depending on the changing CAD were examined. In general, it is understood that the error rate of the results of the standard k- ϵ turbulence model is lower and 3 mm mesh size can be used as the upper limit. It can be said that the error rate of RNG models is better only in the indicated specific fuel consumption data, but in the standard k- ϵ model, the error rates in this data remain in the range of 2-3% and give quite acceptable results.

Evaluations and recommendations within the scope of the studies carried out are stated in the following.

- When experimental data and analysis results are compared, the Standard k- ϵ turbulence model with 2 mm mesh size gives the best results compared to other models, except for the indicated specific fuel consumption.
- Again, in this model, the indicated specific fuel consumption has an accuracy rate of 96% when comparing experimental data and analysis results.
- In the analysis models compared, it is seen that the indicated engine power is also low in the analysis results because the mass gas flow rate is lower than the experimental data.
- When the analysis results are compared, the in-cylinder temperature and pressure values are close in the RNG k- ϵ turbulence models with 2 mm and 3 mm mesh sizes.
- 3 mm mesh size minimized the computation time, while the most accurate results were obtained with a 2 mm mesh size. However, it was concluded that the 3 mm mesh size could also be a viable choice to reduce the computation time by half.
- The importance of the analysis study is understood from this study, as it gives an infinite variation in the desired direction after an experimental verification and saves both cost and time compared to the experimental study.

- For various alternative fuels, intake port, exhaust port, combustion chamber, etc., flow and combustion simulations can be done by using CFD model with changes that may affect engine performance.
- The research highlights the influence of turbulence models and mesh size variations on performance predictions, offering new insights into model selection for two-stroke engine CFD studies. A key contribution is the systematic evaluation of turbulence models and mesh refinements, which has not been extensively analyzed in prior studies. The integration of experimentally measured time-dependent boundary conditions (pressure profiles) in the CFD model enhances accuracy, a step beyond conventional static boundary assumptions.
- The use of boundary conditions with fixed values, such as constant wall temperatures, and simplifications like RANS turbulence models, may not fully capture the transient phenomena in two-stroke engines. As a result, these approximations can lead to deviations from experimental results.

In future studies, the validated CFD approach can be applied to the study of alternative fuels, such as biofuels, hydrogen-enriched blends, and synthetic aviation fuels, to evaluate their impact on combustion efficiency, fuel consumption, and emissions reduction.

Modifications to intake and exhaust port geometries, combustion chamber design, and injection strategies can be analyzed using the CFD model to optimize engine performance.

The use of fixed boundary conditions (e.g., constant wall temperatures) and simplifications like RANS turbulence models may introduce deviations from experimental results, particularly in transient flow conditions. Future studies could explore LES (Large Eddy Simulation) or hybrid RANS-LES approaches for a more detailed analysis of turbulence effects in two-stroke engines.

The proposed simulation framework can be extended to other two-stroke applications, including marine, generator, and high-performance motorcycle engines, to enhance their environmental performance and efficiency.

CONFLICT OF INTEREST

Authors state that they have no conflicts to disclose.

AUTHORS CONTRIBUTION

Gokhan Coskun: Supervision, Methodology, Resources, Writing – original draft. **Yusuf Delil:** Conceptualization, Software, Investigation, Validation. **Usame Demir:** Writing – review & editing, Supervision, Visualization

REFERENCES

Abdulnaser, S. (2009). *Computational Fluid Dynamics*. Venus Publication.

- Aguerre, H. J., Pedreira, P. H., Orbaiz, P. J., & Nigro, N. M. (2022). Validation and enhancement of a supermesh strategy for the CFD simulation of four-stroke internal combustion engines. *Fluids*, 7(3), 104. <https://doi.org/10.3390/FLUIDS7030104>
- Barros, G. F., Grave, M., Viguerie, A., Reali, A., & Coutinho, A. L. G. A. (2022). Dynamic mode decomposition in adaptive mesh refinement and coarsening simulations. *Engineering with Computers*, 38(5), 4241–4268. <https://doi.org/10.1007/S00366-021-01485-6/FIGURES/24>
- Benini, E. (2011). *Advances in gas turbine technology*. IntechOpen.
- Bozza, F., Tuccillo, R., & De Falco, D. (1995). A two-stroke engine model based on advanced simulation of fundamental processes. *SAE Technical Papers*. <https://doi.org/10.4271/952139>
- Cantore, G., Mattarelli, E., & Rinaldini, C. A. (2014). A new design concept for 2-stroke aircraft diesel engines. *Energy Procedia*, 45, 739–748. <https://doi.org/10.1016/J.EGYPRO.2014.01.079>
- Cleveland, F.A. (2012). Size effects in conventional aircraft design. *Journal of Aircraft*, 7(6), 483–512. <https://doi.org/10.2514/3.44204>
- Coskun, G., & Pehlivan, H. (2020). Fluid-structure interaction simulation of excess flow valve movement at different operating pressures and gas flow rates. *Journal of Applied Fluid Mechanics*, 14(2), 615–625. <https://doi.org/10.47176/JAFM.14.02.31717>
- Coskun, G., Delil, Y., & Demir, U. (2019). Analysis of an HCCI engine combustion using toluene reference fuel for different equivalence ratios – Comparison of experimental results with CFD and SRM simulations. *Fuel*, 247. <https://doi.org/10.1016/j.fuel.2019.03.046>
- Coskun, G., Demir, U., Yilmaz, N., & Soyhan, H. S. (2017). Computational investigation of combustion and emission characteristics of toluene reference fuel (TRF) mixtures in an HCCI engine using stochastic reactor model. *Journal of the Brazilian Society of Mechanical Sciences and Engineering*, 39(8). <https://doi.org/10.1007/s40430-017-0844-3>
- Demir, U., Coskun, G., Soyhan, H. S., Turkcan, A., Alptekin, E., & Canakci, M. (2022a). Effects of variable valve timing on the air flow parameters in an electromechanical valve mechanism – A cfd study. *Fuel*, 308, 121956. <https://doi.org/10.1016/J.FUEL.2021.121956>
- Demir, U., Coskun, G., Soyhan, H. S., Turkcan, A., Alptekin, E., & Canakci, M. (2022b). Effects of variable valve timing on the air flow parameters in an electromechanical valve mechanism – A cfd study. *Fuel*, 308, 121956. <https://doi.org/10.1016/J.FUEL.2021.121956>
- Epstein, A. H. (2014). Aeropropulsion for commercial aviation in the twenty-first century and research directions needed. *AIAA Journal*, 52(5), 901–911. <https://doi.org/10.2514/1.J052713>
- Faruoli, M., Coclite, A., Viggiano, A., Caso, P., & Magi, V. (2021). A Comprehensive numerical analysis of the scavenging process in a uniflow two-stroke diesel engine for general aviation. *Energies* 2021, 14(21), 7361. <https://doi.org/10.3390/EN14217361>
- Han, Z., & Reitz, R. D. (1995). Turbulence modeling of internal combustion engines using RNG κ - ϵ models. *Combustion Science and Technology*, 106(4–6), 267–295. <https://doi.org/10.1080/00102209508907782>
- Johnson, T. V. (2009). Review of diesel emissions and control. *International Journal of Engine Research*, 10(5), 275–285. <https://doi.org/10.1243/14680874JER04009>
- Korba, P., Balli, O., Caliskan, H., Al-Rabeei, S., & Kale, U. (2023). Thermodynamics, environmental damage cost, exergoeconomic, life cycle, and exergoenvironmental analyses of a JP-8 fueled turbodiesel aviation engine at take-off phase. *Case Studies in Thermal Engineering*, 43, 102806. <https://doi.org/10.1016/J.CSITE.2023.102806>
- Lakhlifi, Y., Daoudi, S., & Boushaba, F. (2018). Dam-Break Computations by a Dynamical Adaptive Finite Volume Method. *Journal of Applied Fluid Mechanics*, 11(6), 1543–1556. <https://doi.org/10.29252/JAFM.11.06.28564>
- Launder, B. E., Morse, A., Rodi, W., & Spalding, D. B. (1973). Prediction of free shear flows: A comparison of the performance of six turbulence models. *NASA. Langley Res. Center Free Turbulent Shear Flows, 1*.
- Li, Y., Alfazazi, A., Mohan, B., Alexandros Tingas, E., Badra, J., Im, H. G., & Mani Sarathy, S. (2019). Development of a reduced four-component (toluene/n-heptane/iso-octane/ethanol) gasoline surrogate model. *Fuel*, 247, 164–178. <https://doi.org/10.1016/J.FUEL.2019.03.052>
- Mikalsen, R., & Roskilly, A. P. (2008). The design and simulation of a two-stroke free-piston compression ignition engine for electrical power generation. *Applied Thermal Engineering*, 28(5–6), 589–600. <https://doi.org/10.1016/J.APPLTHERMALENG.2007.04.009>
- Rulli, F., Barbato, A., Fontanesi, S., & d’Adamo, A. (2021). Large eddy simulation analysis of the turbulent flow in an optically accessible internal combustion engine using the overset mesh technique. *International Journal of Engine Research*, 22(5), 1440–1456. <https://doi.org/10.1177/1468087419896469>
- Sehra, A. K., & Whitlow, W. (2004). Propulsion and power for 21st century aviation. *Progress in Aerospace Sciences*, 40(4–5), 199–235. <https://doi.org/10.1016/J.PAEROSCI.2004.06.003>
- Taylor, S. J. E., Kiss, T., Anagnostou, A., Terstysanzky, G., Kacsuk, P., Costes, J., & Fantini, N. (2018). The CloudSME simulation platform and its applications: A generic multi-cloud platform for developing and executing commercial cloud-based simulations.

- Future Generation Computer Systems*, 88, 524–539.
<https://doi.org/10.1016/J.FUTURE.2018.06.006>
- Tu, J., Yeoh, G. H., & Liu, C. (2018). *Computational fluid dynamics: A practical approach*. In *Computational Fluid Dynamics: A Practical Approach*. Elsevier.
<http://www.sciencedirect.com:5070/book/9780081011270/computational-fluid-dynamics>
- Turesson, M. (n.d.). *Modelling and simulation of a two-stroke engine*.
- Wang, S., & Zhang, F. (2023). Quantitative analysis of heat transfer characteristics and advantages in opposed-piston 2-stroke diesel engines. *Case Studies in Thermal Engineering*, 51, 103629.
<https://doi.org/10.1016/J.CSITE.2023.103629>
- Wang, Y., Megli, T., Haghgoie, M., Peterson, K. S., & Stefanopoulou, A. G. (2002). Modeling and control of electromechanical valve actuator. *SAE Technical Papers*. <https://doi.org/10.4271/2002-01-1106>